Viscous Loss Assessment in Rocket Engines

Homayun Kehtarnavaz,* Douglas E. Coats,† and Anthony L. Dang‡
Software and Engineering Associates, Inc., Carson City, Nevada 89701

The performance losses in rocket nozzles due to the viscous effects have been studied. Special consideration was given to nozzles with high expansion ratios. The formulation of the boundary-layer equations used in this study includes the effects of transverse and longitudinal curvatures. The effects of longitudinal curvature manifest themselves as a centrifugal force term on the mean flow in the boundary layer and also on the turbulent shear stress model. The results indicate that although the longitudinal curvature creates a fairly strong pressure difference across the boundary layer, the effects on the performance are minimal. The results also show that in high expansion ratio nozzles, the viscous layer becomes very "thick" and the traditional boundary-layer assumptions cause significant error in the viscous loss calculations. Improvements to the method of evaluating thrust loss are presented.

Nomenclature

$H(\eta,\zeta)$ = enthalpy
$k(x)$, $k(\zeta)$ = transformed longitudinal curvature, positive for convex and negative for concave surfaces
L = length scale
Pr = Prandtl number
p = pressure
R = radius of longitudinal curvature
Re = Reynolds number
r = radius of transverse curvature
T = thrust
t = $y\cos\phi/r_0$
u,v = velocity components
x,y = coordinate system
δ = boundary-layer thickness
δ^* = displacement thickness
ϵ = eddy viscosity term
$\bar{\epsilon}(x)$ = given by equation
η,ζ = transformed coordinates
θ = momentum thickness
μ = viscosity
ν = kinematic viscosity
ρ = density
τ = shear stress
ϕ = wall angle
ψ = stream function

Superscripts

$'$ = $\partial/\partial\eta$
$''$ = $\partial^2/\partial\eta^2$
$*$ = potential flow, at distance δ^* from the wall
$-$ = modified value

Subscripts

e = at the edge of boundary layer
H = refers to enthalpy
p = at the edge of potential flow
u = refers to velocity
w = at the wall
0 = to the wall

Introduction

THE trend toward very large area ratio nozzles, which result in performance gains for space applications, has increased the need for detailed knowledge of the momentum losses due to nozzle viscous effects (i.e., boundary layer) in propulsion systems. These losses degrade overall system performance by increasing system weight, decreasing useful payload weight, and/or decreasing effective system range. The traditional approaches[1-8] use the Prandtl thin shear-layer approximation, i.e., $\delta/L \ll 1$, to compute the losses due to viscous effects. These assumptions eliminate the normal momentum equation or the centrifugal force balance. The normal pressure gradient vanishes not because the shear layer is thin, but because the surface is relatively flat, i.e., the radius of curvature is large.

Van Dyke[9,10] has shown that longitudinal curvature makes a contribution that is additive to that of transverse curvature and is of the same relative order of magnitude. The perturbation theory applied by Van Dyke demonstrates the importance of second-order terms. The metric influence of curvature has been given by Schultz-Grunow and Brewer[11] for laminar and incompressible flows.

Cebeci et al.[12] analyzed the turbulent boundary layer on a (convex) longitudinally curved surface. In their treatment they replaced the laminar viscosity with an effective eddy viscosity. The eddy viscosity was specified to be the standard Cebeci and Smith[13] formulation modified by Bradshaw's[14] correction for longitudinal curvature. Eghlima and Kleinstreyer[15] used a similar approach. However, in all these approaches, the assumption has been made that the vorticity vanishes along the edge of the boundary layer, i.e., the outer flow is irrotational.

It has been found that the standard Joint Army Navy Air Force (JANNAF) method[2] for predicting boundary-layer losses is not sufficiently accurate for computing boundary-layer losses for space engines. These engines exhibit substantial boundary-layer growth due to their very high expansion ratios. For small engines, a major portion of the nozzle flow can be completely enveloped by the wall shear layer (up to 90%).

The two major deficiencies of the JANNAF boundary-layer thrust loss calculation method[2] are that the effects of both transverse and longitudinal curvature are assumed to be small. Because, in highly expanded flows, the boundary-layer thick-

Received Dec. 9, 1987; revision received Jan. 4, 1990.

*Senior Research Scientist; currently at Physical Research, Inc., Irvine, CA 92718. Member AIAA.
†Vice President. Senior Member AIAA.
‡Principal Research Scientist; currently at Physical Research, Inc., Irvine, CA 92718.

ness can become a significant fraction of either the transverse or longitudinal curvature, this effect should not be ignored. The objective of this paper is 1) to assess the significance of nozzle wall curvature effects, and 2) to assess performance losses due to viscous effects using a more complete description of the viscous shear layer within the boundary-layer equations for a wide range of space applications engines.

Theory

For a compressible boundary-layer flow in an axisymmetric nozzle, the governing equations including the transverse and longitudinal curvature effects are given as the following[12,15,17,18]:
Continuity:

$$\frac{\partial}{\partial x}(\rho u r^n) + \frac{\partial}{\partial y}\left[\overline{\rho v r^n}(1+ky)\right] = 0 \tag{1}$$

Streamwise momentum:

$$\rho\frac{u}{1+ky}\frac{\partial u}{\partial x} + \overline{\rho v}\frac{\partial u}{\partial y} + \frac{\rho k u v}{1+ky} = -\frac{1}{1+ky}\frac{\partial \rho}{\partial x} + \frac{1}{r^n(1+ky)} \cdot \frac{\partial}{\partial y}\left[r^n(1+ky)\left(\mu\frac{\partial u}{\partial y} - \overline{\rho v' u'}\right)\right]; \quad \overline{\rho v} = \rho v + \overline{\rho' v'} \tag{2a}$$

Normal momentum:

$$\frac{k u^2}{1+ky} = \frac{1}{\rho}\frac{\partial p}{\partial y} \tag{2b}$$

Energy:

$$\frac{\rho u}{1+ky}\frac{\partial H}{\partial x} + \overline{\rho v}\frac{\partial H}{\partial y} = \frac{1}{r^n(1+ky)} \cdot \frac{\partial}{\partial y}\left\{r^n(1+ky) \cdot \left[\frac{\mu}{Pr}\frac{\partial H}{\partial y} + \mu\left(1-\frac{1}{Pr}\right)u\frac{\partial u}{\partial y} - \rho\overline{H' v'}\right]\right\} \tag{3}$$

The influence of longitudinal curvature on the mean boundary-layer flow is modeled by inclusion of the centrifugal force term in the normal momentum equation[9-11] [see Eq. (2b)].

Figure 1 shows the definition of r, r_0, R_0, and R.

Transverse curvature is defined as

$$t = (y\cos\phi/r_0) = r/r_0 \tag{4a}$$

and the longitudinal curvature as

$$(1/R_0) = k(x) \tag{4b}$$

and

$$(R/R_0) = 1 + k(x)y \tag{4c}$$

The boundary conditions for Eqs. (1-3) are at

$$y = 0, \qquad u = 0, \qquad v = v_w(x), \tag{5a}$$

and

$$T = T_w(x) \quad \text{or} \quad \dot{q}_w(x) \tag{5b}$$

is known at

$$y = y_{\max}, \qquad u = u_e, \qquad H = H_e$$

$$p = p_e + (\rho_e k/1+ky)\, u_e^2 y_{\max} \tag{5c}$$

The boundary condition for $p(y_{\max})$ was taken from Van Dyke[9,10] who matched the inner limit of the outer expansion jth iteration to the $(j-1)$th iteration of the inner flow (i.e., the boundary layer). Van Dyke showed that Eqs. (2a) and (5c) include all second-order terms caused by longitudinal curvature effect.

To include the longitudinal curvature effect in the eddy viscosity model, Bradshaw's[19] expression has been employed to correct the inner eddy viscosity term by multiplying this expression by S^2 where

$$S = \frac{1}{1+R_i\beta} \qquad R_i = 2u\,k(u)\left(\frac{\partial u}{\partial y}\right)^{-1} \tag{6}$$

where R_i is analogous to Richardson number and β is reported to be 7 for convex and 4 for concave surfaces.[19]

The streamwise momentum equation, [Eq. (2a)], requires $\partial p/\partial x$ along lines of constant y.

Surfaces of constant η are all parallel to the curved wall. At the boundary-layer edge, the term $(\partial p/\partial x)_y$ is given by:

$$\left(\frac{\partial p}{\partial x}\right)_y = -\rho_e u_e \frac{du_e}{dx} + \left(\frac{\partial p}{\partial y}\right)_x\left(\frac{\partial y}{\partial \eta}\right)_x\left(\frac{\partial \eta}{\partial x}\right)_y \tag{7}$$

The conventional JANNAF method[2] for evaluation of the viscous thrust loss in rocket engine nozzle employs both the boundary-layer momentum and displacement thicknesses. This method can be arrived at by two different approaches as shown by Alber.[20] The basis for the approach is to compare the thrust of an inviscid nozzle to a viscous nozzle with the same mass flow rate. In Eq. (8) the first term represents the pressure forces acting on an inviscid nozzle and the second and third terms represent the total stress forces acting on the viscous nozzle.

$$\Delta T = \int_0^S \left(p_e^* - p_\infty\right)2\pi r_p \frac{dr_p}{dx} - \int_0^S \left(p_w - p_\infty\right)2\pi\left(r_p + \bar{\delta}^*\cos\phi\right) \cdot \frac{d(r_p + \bar{\delta}^*\cos\phi)}{dx}\,dx + \int_0^S \tau_w 2\pi\left(r_p + \bar{\delta}^*\cos\phi\right)\cos\phi\, dx \tag{8}$$

where r_p is the distance from the axis to the potential wall and p_e^* the pressure at r_p, as shown in Fig. 1. For thin boundary layers, the conventional assumption is to let $r_p = r_0$. However, to maintain generality, Eq. (8) distinguishes between the potential and real wall. The integral form of the momentum equation (with transverse and longitudinal curvature effects) can be derived as

$$\frac{\partial}{\partial x}\left[\rho_e u_e^2 r_0 \int_0^\delta \frac{r}{r_0}\frac{\rho u}{\rho_e u_e}\left(1-\frac{u}{u_e}\right)dy\right] + \rho_e u_e r_0 \frac{\partial u_e}{\partial x}\int_0^\delta \left(1-\frac{\rho u}{\rho_e u_e}\right)\frac{r}{r_0}\,dy - r_0\int_0^\delta \frac{r}{r_0}\rho k u v\,dy - \epsilon(x) r_0\left(\delta - \frac{\delta 2}{2r_0}\right) = \tau_w r_0 \tag{9a}$$

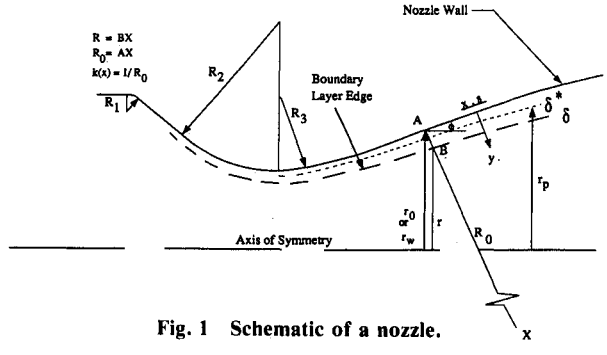

Fig. 1 Schematic of a nozzle.

where

$$\frac{\partial p_e}{\partial x} + \rho_e u_e \frac{\partial u_e}{\partial x} = \epsilon(x) \tag{9b}$$

The details of the derivation can be found in Ref. 16. Alternate forms of the momentum and displacement thicknesses for axisymmetric flows are defined as

Momentum thickness:

$$\bar{\theta} = \int_0^{\delta} \frac{r}{r_0} \frac{\rho u}{\rho_e u_e} \left(1 - \frac{u}{u_e}\right) dy \tag{10a}$$

Displacement thickness:

$$\bar{\delta}^* = \int_0^{\delta} \frac{r}{r_0} \left(1 - \frac{\rho u}{\rho_e u_e}\right) dy \tag{10b}$$

Implementing Eqs. (9b), (10a), and (10b) into Eq. (9a) yields

$$\frac{\partial}{\partial x}\left(\rho_e u_e^2 r_0 \bar{\theta}\right) - r_0 \bar{\delta}^* \frac{\partial \rho_e}{\partial x} - r_0 \int_0^{\delta} \frac{r}{r_0} \rho k u v \, dy + \epsilon(x) r_0 \left[\bar{\delta}^* - \delta + \frac{\delta^2}{2r_0}\right] = \tau_w r_0 \tag{11}$$

Inserting Eq. (11) in Eq. (8) and neglecting terms of order $\bar{\delta}^{2*}$, the thrust deficit is

$$\frac{\Delta T}{2\pi} = \int_0^S \left[p_e^* - p_w\right] r_p \frac{dr_p}{dx} dx - \int_0^S \left[p_w - p_\infty\right] \frac{d}{dx}\left(r_p \bar{\delta}^* \cos\phi\right) dx + \int_0^S r_0 \left[-k(x) \int_0^{\delta} \frac{r}{r_0} \rho u v \, dy + \epsilon(x)\left(\bar{\delta}^* - \delta + \delta^2/2r_0\right)\right] \cdot \cos\phi \, dx + \int_0^S \cos\phi \cdot \left[\frac{\partial}{\partial x}\left(\rho_e u_e^2 r_0 \bar{\theta}\right) - r_0 \bar{\delta}^* \frac{\partial}{\partial x}\left(p_e - p_\infty\right)\right] dx \tag{12}$$

Here p_e^* is the pressure at the edge of the potential flow and p_e the pressure at the edge of the boundary layer, i.e., at $r_w - \delta \cos\phi$.

To this point, the thrust loss equation has been derived with very few of the traditional boundary-layer assumptions being made. To examine the effects of these assumptions, they will be applied one at a time.

1) Nondissipative edge condition, i.e., $\epsilon(x) \neq 0$. In the absence of dissipative or applied forces on the core flow, Bernoulli's equation is satisfied and $\epsilon(x) = 0$ [see (Eq. 9b)]. Examples of flows where $\epsilon(x) \neq 0$ would be two phase core flow or magnetohydrodynamic (MHD) flow. The second term of the third integral in Eq. (12) disappears when $\epsilon(x) = 0$.

2) The boundary layer is thin compared to the local radius of curvature, i.e., $\delta/R_0 \langle\langle 1$. This assumption leads to the following:

$$\partial p/\partial y = 0 \qquad \text{or} \qquad p = p_w = p_e^* = p_e$$

and

$$\partial \phi/\partial x = 0$$

$$\frac{\Delta T}{2\pi} = \int_0^S \cos\phi \cdot \frac{\partial}{\partial x}\left[\rho_e u_e^2 r_0 \bar{\theta} - r_0 \bar{\delta}^* \left(p_e - p_\infty\right)\right] dx - \int_0^S \left(p_e - p_\infty\right) \cos\phi \frac{d}{dx}\left(r_p \bar{\delta}^*\right) dx \tag{13}$$

Integrating the first term in Eq. (13) by parts and assuming that $\bar{\delta}^*(s=0) = \bar{\theta}(s=0) = 0$ yields

$$\frac{\Delta T}{2\pi} = \rho_e u_e^2 r_p \bar{\theta} \cos\phi - r_p \bar{\delta}^* \left(p_e - p_\infty\right) \cos\phi - \int_0^S \rho_e u_e^2 r_0 \bar{\theta} \cos\phi \frac{\partial}{\partial x}\left(\frac{r_p}{r_0}\right) dx \tag{14}$$

3) For adiabatic and cooled wall flows, the displacement thickness $\bar{\delta}^*$ is usually less than the boundary-layer thickness δ. The assumption applied here is that $\bar{\delta}^* \cos\phi / r_p \ll 1$, which is less restrictive than $\delta/r_p \ll 1$. The remaining integral in Eq. (14) vanishes by noting that

$$r_p/r_0 = 1(\bar{\delta}^*/r_0) \cos\phi = 1$$

To the same order of accuracy, Eq. (14) can be rewritten as

$$(\Delta T/2\pi) = \rho_e u_e^2 r_0 \bar{\theta} \cos\phi - r_0 \bar{\delta}^* (p_e - p_\infty) \cos\phi \tag{15}$$

4) Equation (15) reduces to the standard JANNAF[2] relationship for thrust loss with the additional assumption $\delta \cos\phi / r_0 \ll 1$. That is,

$$\frac{r}{r_0} = 1 - \frac{\delta \cos\phi}{r_0} \simeq 1$$

which leads to

$$\theta = \bar{\theta} \qquad \text{and} \qquad \delta^* = \bar{\delta}^*$$

and Eq. (15) becomes

$$\Delta T = 2\pi \cos\phi \left[\rho_e u_e^2 r_0 \theta - r_0 \delta^* (p_e - p_\infty)\right] \tag{16}$$

In conclusion, it can be seen that in order to reduce the general form of the thrust loss Eq. (8) to the standard JANNAF form,[2] i.e., Eq. (16), requires four assumptions. The first assumption, i.e., that Bernoulli's equation is satisfied at the edge of the boundary layer is met in most liquid rocket engines of interest.

The other three assumptions deal with varying degrees of how thin the boundary layer is compared to a given length scale. The "thin" assumptions are the following:

1) The boundary layer is thin compared to the local longitudinal radius of curvature, i.e., $\delta/R_0 \ll 1$.

2) The displacement between the viscous and potential walls is small compared to the local wall radius, i.e., $\bar{\delta}^* \cos\phi / r_0 \ll 1$, which leads to $r_p \simeq r_0$.

3) The boundary-layer thickness is small compared to the local wall radius, i.e., $\delta \cos\phi / r_0 \ll 1$, which leads to $r \simeq r_p \simeq r_0$.

Results and Discussion

The BLM (boundary layer module) within the TDK (two-dimensional kinetics) code was modified to include the normal momentum equation together with longitudinal curvature terms.

Solutions to the momentum and energy equations can be obtained in a very efficient manner by using the block elimination method as discussed by Keller. The implicit finite difference scheme that has been developed by Keller and Cebeci[21] was implemented to obtain numerical solution to these equations.[16] The BLM code was validated by comparison to another boundary-layer code, MABL.[22] The code was also verified for flow over a flat plate and available experimental data for flow over a convex surface. These results are presented in Ref. 16.

The nozzle wall is not generally known analytically and is often obtained from tabular input data by spline fitting. Calculation of longitudinal curvature that requires the second derivative of a nozzle wall creates severe fluctuations of the second derivative, which in turn can cause numerical instabilities. It was decided to divide the nozzle wall into numbers of equally spaced intervals and let a circle pass through every three points. The radius of the circle is taken to be the radius of the curvature at the middle point. This method has been verified against an analytical wall and the results are satisfactory.[16]

Table 1 Boundary-layer thrust deficit for variety of engines in the absence and presence of the longitudinal curvature (cold wall case)

	Thrust deficit, lbf s/lbm									
	Without longitudinal curvature					With longitudinal curvature				
Nozzle	Eq. (A)	Eq. (B)	Eq. (C)	Eq. (D)	Eq. (E)	Eq. (A)	Eq. (B)	Eq. (C)	Eq. (D)	Eq. (E)
SSME	6.8843	6.7730	6.7650	6.2088	6.2233	6.3720	6.3184	6.4758	6.0387	6.5036
ASE	14.1985	13.6977	13.4572	12.3531	11.9394	14.2351	13.7440	13.5000	12.3782	11.7659
RL-10	11.6549	11.0871	10.8094	10.4630	10.4930	11.7732	11.0714	10.8591	10.4517	10.4964
XDELTA[a]	1.8459	1.8160	1.7902	1.7220	1.8132	1.8459	1.8160	1.7870	1.7215	1.8211
BC4515[b]	0.8688	0.8534	0.8481	0.8142	0.8373	0.8686	0.8534	0.8221	0.8141	0.8378
BC1010[b]	1.8578	1.7941	1.7866	1.8000	1.8790	1.8582	1.7942	1.8121	1.8001	1.8788
IUS	1.9864	1.9523	1.9223	1.8381	2.0943	1.9862	1.9521	1.8524	1.8380	2.0828
XLR-134	27.3282	25.6350	25.3452	24.8578	23.2534	27.3525	25.6539	25.2531	24.6322	23.1904

Eq. (A) $\Delta T = 2\pi \cos\phi\ [\rho_e u_e^2 r_0 \theta - r_0 \delta^* (p_e - p_\infty)]$

Eq. (B) $\Delta T = 2\pi [\rho_e u_e^2 r_0 \bar{\theta} \cos\phi - r_0 \bar{\delta}^* (p_e - p_\infty) \cos\phi]$

Eq. (C) $\Delta T = 2\pi [\rho_e u_e^2 r_p \bar{\theta} \cos\phi - r_p \bar{\delta}^* (p_e - p_\infty) \cos\phi]$

Eq. (D) $$\Delta T = 2\pi \left[\rho_e u_e^2 r_p \bar{\theta} \cos\phi - r_p \bar{\delta}^* \left(p_e - p_\infty \right) \cos\phi - \int_0^S \rho_e u_e^2 r_0 \bar{\theta} \cos\phi \frac{\partial}{\partial x} \left(\frac{r_p}{r_0} \right) dx \right]$$

Eq. (E) $$\Delta T = \int_0^S \left(p_e^* - p_\infty \right) 2\pi r_p \frac{dr_p}{dx}\, dx - \int_0^S \left(p_w - p_\infty \right) 2\pi \frac{\partial}{\partial x} \left(r \bar{\delta}^* \cos\phi \right) dx + \int_0^S \tau_w 2\pi \left(r_p + \bar{\delta}^* \cos\phi \right) \cos\phi\, dx$$

where $\bar{\epsilon}(x) = 0$

[a]Extended delta (solid propellant space motor). [b]Experiment nozzles by Jet Propulsion Lab., cone-shaped.

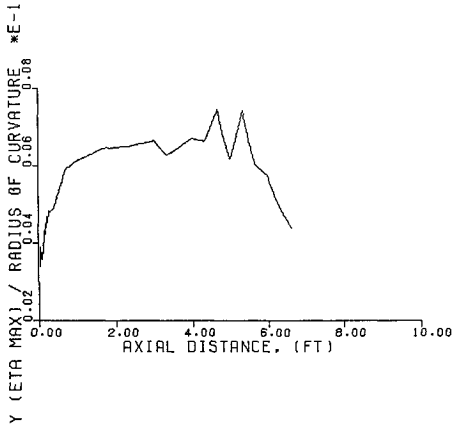

Fig. 2a Magnitude of δ/R_0 for ASE nozzle.

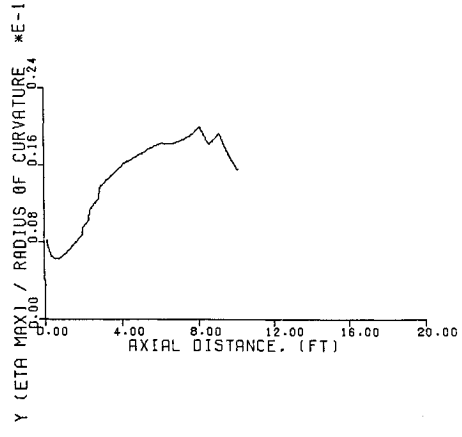

Fig. 2b Magnitude of δ/R_0 for SSME nozzle.

The importance of longitudinal curvature is determined by the magnitude of δ/R_0, i.e., the ratio of the boundary-layer thickness to the radius of curvature. Figures 2a and 2b indicate this value for Rocketdyne Advance Space Engine (ASE) and Space Shuttle Main Engine (SSME) nozzles, respectively. The magnitude of δ/R_0 for SSME is larger than ASE nozzle and thus a larger pressure gradient across the boundary layer is expected. This can be observed from a comparison of velocity profiles in Figs. 3 and 4.

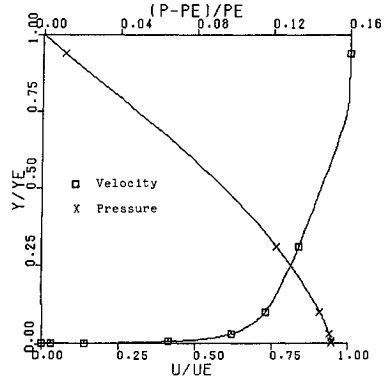

Fig. 3 Velocity and pressure profiles for ASE nozzle at the exit plane.

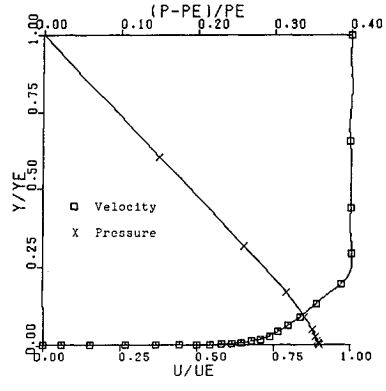

Fig. 4 Velocity and pressure profiles for SSME nozzle at the exit plane.

The effect of longitudinal curvature on performance is depicted in Table 1. It can be seen that although the longitudinal curvature affects the mean flow velocity, temperature, and pressure profiles in the boundary layer, it has insignificant

impact on nozzle performance. However, the methodology being used to evaluate viscous loss has to distinguish between a thin and thick boundary layer.

Essentially, Table 1, Eq. (A), which is the standard JANNAF method, is not valid for thick boundary layers because of the magnitude of term r/r_0, where r is the distance from the axis of symmetry to the edge of the boundary layer. As the value of r/r_0 increases, the thin shear-layer assumption yields erroneous results for boundary-layer losses, i.e., Table 1, Eq. (A). Table 1, Eq. (B) was developed for axisymmetric flows, and for the thick boundary layers is expected to yield quite different values from Table 1 Eq. (A). It can be seen that for nozzles with high area ratio such as ASE, RL-10 (Pratt Whitney Space Engine) and XLR134 (orbital transfer vehicle engine, space storable), the difference between these equations is more significant. This difference is due to a thick boundary layer when r/r_0 is significantly less than unity. To be more exact, r_p should be replaced for r_0 in Table 1, in Eq. (B), as shown in the analysis; upon doing that, the effects are more severe on the high area ratio nozzles, Table 1, Eq. (C). The results of adding another higher order term to Table 1, Eq. (C) has been indicated in Table 1, Eq. (D). It can be seen that addition of this term makes a change of up to about 8% in the thrust loss for high area ratio nozzles. Using the integrated wall shear method, i.e., Table 1, Eq. (E), yields results quite different (up to 16%) from Table 1, Eq. (A) for ASE nozzle (area ratio = 400), RL-10 (area ratio 205), and XLR134 (area ratio 767:1). However, as the higher order terms are added to Table 1, Eq. (D), the results become closer to values of Table 1, Eq. (E). This is expected because of mathematical equivalency of both equations. The overall results indicate that the standard JANNAF method for performance prediction is not adequate and can produce fairly large error performance predictions for high expansion nozzles.

The results indicated in this table justify the usage of Table 1, Eq. (E) for the thrust calculations and Table 1, Eq. (E) should be used to obtain the thrust loss. Furthermore, the inclusion of longitudinal curvature is not crucial to performance prediction in a contoured wall of a rocket engine nozzle.

Concluding Remarks

The results in this work indicated that although the effects of the longitudinal curvature are of importance on the mean flow velocity, pressure, and temperature profiles in the boundary layer in strongly curved nozzle contours, it does not have a significant impact on the overall prediction of nozzle performance. However, for nozzles with a thick viscous layer, the standard JANNAF method that is formulated for thin shear layers overestimates the boundary-layer thrust deficit and it should be replaced by the Table 1, Eq. (E), which will be referred to as wall shear method.

Acknowledgments

This work was performed at Software and Engineering Associates, Inc., under Astronautics Laboratory (AFAL) Contract F0411-86-C-0055. The authors wish to thank Phillip Kessel and Elizabeth Slimak at AFA for their support.

References

[1]Pieper, J. L., "Performance Evaluation Methods for Liquid Propellant Rocket Thrust Chambers," Chemical Propulsion Information Agency, Applied Physics Lab., Laurel, MD, CPIA Pub. 132, prepared for the Performance Standardization Working Group, Nov. 1966.

[2]"JANNAF Rocket Engine Performance Prediction and Evaluation Manual," Chemical Propulsion Information Agency, Applied Physics Lab., Laurel, MD, CPIA Pub. 246, April 1975.

[3]Nickerson, G. R., Dang, L. D., and Coats, D. E., "Two-Dimensional Kinetics (TDK) Reference Computer Program," Software and Engineering Associates, Inc., Carson City, NV, Final Rept. NASA Contract NAS8-35931, April 1985.

[4]Nickerson, G. R., Coats, D. E., Hermsen, R. W., and Lamberty, J. T., "A Computer Program for the Prediction of Solid Propellant Rocket Motor Performance (SPP)," Vol. 1, Software and Engineering Associates, Inc., Carson City, NV, AFRPL TR-83-036, Sept. 1984.

[5]Weingold, H. D., "The ICRPG Turbulent Boundary Layer (TBL) Reference Program," ICRPG Performance Standarization Working Group, July 1968.

[6]Evans, M., *BLIMP-J User's Manual,* Aerotherm Division/Acurex Corporation, Contract NAS8-30930, July 1975.

[7]Cebeci, T., "Boundary Layer Analysis Module," Software and Engineering Associates, Inc., Carson City, NV, Jan. 1982.

[8]Landau, L. D., and Lifshitz, E. M., *Fluid Mechanics,* Pergamon, London, 1959, Chap. 2, p. 79.

[9]Van Dyke, M., "Higher Approximation in Boundary Layer Theory, Part 1, General Analysis," *Journal of Fluid Mechanics*, 1962, p. 161.

[10]Van Dyke, M., "Higher-Order-Boundary-Layer Theory," *Annual Review of Fluid Mechanics,* 1969, p. 265.

[11]Schultz-Grunow, F., and Breuer, W., "Laminar Boundary Layers on Cambered Walls," *Basic Developments in Fluid Mechanics,* Vol. 1, Academic, New York, 1965, p. 377.

[12]Cebeci, T., Hirsh, R. S., and Whitelaw, J. H., "On the Calculation of Laminar and Turbulent Boundary Layers on Longitudinally Curved Surfaces," *AIAA Journal,* Vol. 17, No. 4, 1979, p. 434.

[13]Cebeci, T., and Smith, A. M. O., *Analysis of Turbulent Boundary Layers,* Academic, New York, 1974.

[14]Bradshaw, P., "The Analogy Between Streamline Curvature and Buoyancy in Turbulent Shear Flow," *Journal of Fluid Mechanics,* Vol. 36, Pt. 1, 1969, pp. 177–191.

[15]Eghlima, A., and Kleinstreuer, C., "Numerical Analysis of Attached Turbulent Boundary Layers Along Strongly Curved Surfaces," *AIAA Journal*, Vol. 23, No. 2, 1985, p. 177.

[16]Kehtarnavaz, H., Coats, D. E., Nickerson, G. R., and Dang, A. L., "Two-Dimensional Kinetics (TDK) Nozzle Performance Computer Program—Thick Boundary Layer Version," Software and Engineering Associates, Inc., Carson City, NV, Rept. AFAL-TR-87-031, March 1987.

[17]Cebeci, T., "Eddy-Viscosity Distribution in Thick Axisymmetric Turbulent Boundary Layers," *Journal of Fluid Engineering*, June 1973, No. 95, p. 319.

[18]So, R. M. C., "Momentum Integral for Curved Shear Layers," *Journal of Fluid Engineering,* June 1975, p. 253.

[19]Bradshaw, P., "The Analogy Between Streamline Curvature and Buoyancy in Turbulent Shear Flow," *Journal of Fluid Mechanics,* Vol. 36, Pt. 1, 1969, pp. 177–191.

[20]Alber, E. I., "Comparison and Evaluation of Computer Program Results for Rocket Engine Performance Prediction. Chap. V, Boundary Layer Friction and Heat Transfer," Dynamic Science for Interagency Chemical Rocket Propulsion Group, CN NAS 7-443 NS-82, 1968.

[21]Keller, H. B., and Cebeci, T., "Accurate Numerical Methods for Boundary Layer Flows, Part II, Two-Dimensional Turbulent Flows," *AIAA Journal*, Vol. 10, 1972, p. 1193.

[22]Dang, A. L., Kehtarnavaz, H., and Nickerson, G. R., "Solution of the Boundary Layer Equations with Non-Equilibrium Reacting Chemistry in Rocket Nozzels," 25th Joint Army Navy NASA Airforce Combustion Meeting, NASA Marshall Space Flight Center, Huntsville, AL, Oct. 1988.